groups proximate to it, and an ester group unfavorably influences the hydrolysis of an adjacent acid fluoride unit. This effect may be a steric one. At a low content of MF units, each MF unit in the MF–MMA copolymer is isolated by MMA units, where the (MMA–MF–MMA) configuration is predominant. The MF units in (MMA–MF–MMA) triads are considered to hydrolyze much more slowly than in the (MF–MF) dyad, since the rate constants were 11–23 times lower for copolymer 2 than for copolymer 8 (Table II).

As mentioned in the preceding section, the hydrolysis of the MF–MMA copolymers involves two mechanisms, an externally catalyzed hydrolysis and an internal hydrolysis with participation of adjacent groups. The results of the infrared measurements indicate that the hydrolysis of MMA units in the early stage of the reaction is practically negligible in comparison to that of the MF units, since the intensities of ester carbonyl bands remained almost unchanged until late in the reaction. Thus, the reaction occurred exclusively at the (MF–MF) configurations. An anhydride formation reaction between different polymeric chains seems unlikely if one considers the dilution of the medium and the solubility of the products in organic solvents. Therefore, the reaction mechanism in the initial stage is formulated as follows:

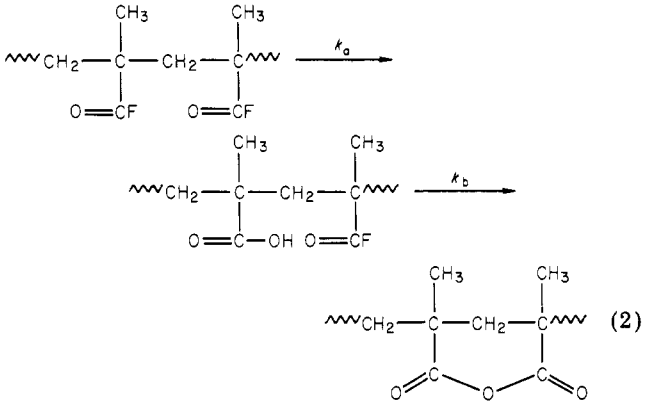

(2)

The initial hydrolysis of an acid fluoride unit is the rate-determining step in the reaction sequence; i.e., $k_a < k_b$, since any absorption due to carboxylic acid groups was not observed in the infrared spectra of the products at a low degree of hydrolysis.

At a late stage the hydrolyzed copolymers were precipitated, in part, from the reaction mixture, and the hydrolysis rate decreased gradually, giving first-order plots with a downward curvature. The infrared analysis revealed the presence of methacrylic acid units in the products at a high degree of hydrolysis.

It may be concluded that the hydrolysis rate of MF units in the MF–MMA copolymers depends on their respective microstructures, especially on their number fraction of (MF–MF) sequences. The findings suggest that the rate of fluoride ion release from MF–MMA copolymers can be made to vary by changes in their configurations even at a constant content of MF units in the copolymers: the rate would be highest for MF–MMA block copolymer and lowest for MF–MMA alternating copolymer.

References and Notes

(1) Retief, D. H.; Sorvas, P. G.; Bradley, E. L.; Taylor, R. E.; Walker, A. R. *J. Dent. Res.* **1980**, *59*, 573.
(2) Fogels, H. R.; Alman, J. E.; Meade, J. J.; O'Donnell, J. P. *J. Am. Dent. Assoc.* **1979**, *99*, 456.
(3) Ringelberg, M. L.; Webster, D. B.; Dixon, D. O.; LeZotte, D. C. *J. Am. Dent. Assoc.* **1979**, *98*, 202.
(4) Kadoma, Y.; Masuhara, E.; Ueda, M.; Imai, Y. *Makromol. Chem.* **1981**, *182*, 273.
(5) Smets, G.; Van Humbeeck, W. *J. Polym. Sci., Part A* **1963**, *1*, 1227.
(6) Smets, G.; De Loecker, W. *J. Polym. Sci.* **1959**, *41*, 375.
(7) Smets, G.; De Loecker, W. *J. Polym. Sci.* **1960**, *45*, 461.
(8) Glavis, F. J. *J. Polym. Sci.* **1959**, *36*, 547.
(9) Smets, G. *Angew. Chem.* **1962**, *74*, 337.
(10) Smets, G.; Hous, P.; Deval, N. *J. Polym. Sci., Part A* **1964**, *2*, 4825.
(11) Matsuzaki, K.; Okamoto, T.; Ishida, A.; Sobue, H. *J. Polym. Sci., Part A* **1964**, *2*, 1105.
(12) Sakurada, I.; Iwagaki, T.; Sakaguchi, Y. *Kobunshi Kagaku* **1964**, *21*, 270.
(13) Chapman, C. B. *J. Polym. Sci.* **1960**, *45*, 237.
(14) Ito, K.; Yamashita, Y. *J. Polym. Sci., Part A* **1965**, *3*, 2165.

Tensile and Swelling Behavior of Model Silicone Networks with Low Extents of Cross-Linking

Kenneth A. Kirk, Susan A. Bidstrup, Edward W. Merrill, and Kevin O. Meyers*

Department of Chemical Engineering, Massachusetts Institute of Technology, Cambridge, Massachusetts 02139. *Received July 8, 1981*

ABSTRACT: Multifunctional elastomeric networks of known network chain density, ν_s/V, were prepared by end-linking α,ω-divinyl-poly(dimethylsiloxane) (α,ω-divinyl-PDMS) chains ranging in number-average molecular weight from 9320 to 28 100 with poly(methylsiloxane) (PMHS) of average intrinsic functionality 43.9. The fraction of silane vinyls reacted, ϵ, as measured from sol fraction analysis, varied from 0.95 to 0.4. The stress–strain isotherms in elongation and the swelling ratios in benzene were measured at 25 °C for these networks. Network chain densities calculated from these measurements exceeded the values predicted from stoichiometry. These excesses diminished with decreasing ϵ. Molecular theories presuming a contribution from trapped entanglements to the small-strain modulus gave good agreement with the data and offered a reasonable explanation of the trends observed.

In previous papers,[1,2] the equilibrium tensile behavior of model silicone elastomeric networks with high junction functionalities was described. Such high-functionality networks were prepared by reacting the terminal vinyl groups on α,ω-divinyl-poly(dimethylsiloxane) (α,ω-divinyl-PDMS) chain molecules with the silane hydrogens on poly(methylsiloxane) (PMHS):

*To whom correspondence should be addressed at ARCO Oil and Gas Co., Production Research Center, Dallas, Texas 75221.

0024-9297/82/2215-1123$01.25/0

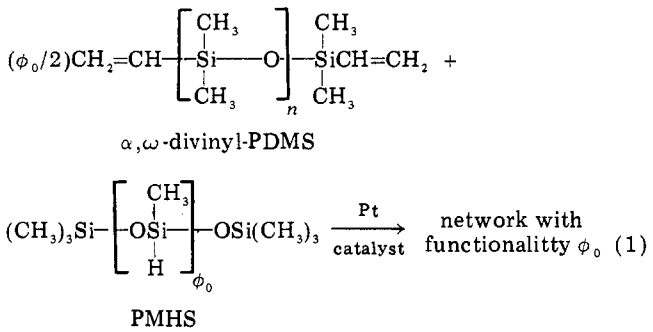

By employing this end-linking reaction, one may calculate the concentration of network chains, ν_s/V, from the known molecular weight of the α,ω-divinyl-PDMS. The functionality ϕ_0 is likewise governed by the molecular weight of the PMHS polymer used. Networks with high junction functionality are predicted to display unique tensile behavior (vide infra), facilitating evaluation of the various molecular theories of rubber elasticity. The previous studies[1,2] dealt with high-functionality networks formed under conditions such that the end-linking reaction was driven to near completion. In those networks the fraction of terminal vinyl groups reacted, ϵ, was greater than 0.90. The current study deals with high-functionality networks formed such that ϵ ranges from 0.4 to 0.95.

Theory

The elastic modulus for uniaxial extension $[f]$ may be defined as

$$[f] = f/[A(\alpha - \alpha^{-2})] \quad (2)$$

where f is the applied load, A is the undeformed cross-sectional area, and α is the extension ratio given by

$$\alpha = L/L_i \quad (3)$$

Here, L is the length of the elongated sample and L_i is the undeformed length at volume V of the undeformed sample. For moderate extension, the elastic modulus is experimentally correlated with α by the well-known Mooney–Rivlin[3] equation:

$$[f] = 2C_1 + 2C_2\alpha^{-1} \quad (4)$$

where C_1 and C_2 are constants independent of strain.

The dependence of the elastic modulus on strain diverges from the classical molecular theories of rubber elasticity, which predict the elastic modulus to be constant over the entire range of deformation.[4,5] To explain this divergence Flory[6] and Ronca and Allegra[7] have separately proposed a new model based on the hypothesis that in a real network, the fluctuations of a junction about its mean position may be significantly impeded by interactions with chains emanating from spatially, but not topologically, neighboring junctions. Thus, the junctions in a real network are more constrained than those in a network in which the chains are presumed to be devoid of all material character, i.e., "phantom" in nature. Thus the elastic modulus is taken to be the sum of two contributions:

$$[f] = [f_{ph}] + [f_c] \quad (5)$$

f_c is the additional force arising from the aforementioned constraints on junction fluctuations and f_{ph} is the force predicted by the phantom network theory:[5]

$$[f_{ph}] = \nu kT(V/V_0)^{2/3}(1 - 2/\phi)/V \quad (6)$$

where T is the absolute temperature, k is the Boltzmann constant, V_0 is the volume in the undeformed state such that the mean-squared end-to-end length $\langle r^2\rangle$ of a chain assumes the value $\langle r^2\rangle_0$ for unperturbed, free chains, ν is the number of chains, V is the volume of the network, and ϕ is the network functionality. Thus eq 5 may be rewritten as

$$[f] = (1 - 2/\phi)\nu kT(V/V_0)^{2/3}(1 + f_c/f_{ph})/V \quad (7)$$

wherein f_c/f_{ph} is dependent on strain.

The Flory theory[6] predicts that in simple elongation the ratio f_c/f_{ph} decreases with increasing strain and eventually goes to zero as α goes to infinity (phantom network). Furthermore, at $\alpha = 1$, the theory holds that

$$f_c/f_{ph} \leq 2/(\phi - 2) \quad (8)$$

The equality is only obtained in eq 8 for the extreme limit in which the junction fluctuations are totally suppressed. The theory reduces to the affine deformation model in that limit:

$$[f] = \nu kT(V/V_0)^{2/3}/V \quad (9)$$

The theory also predicts that as the functionality of a network (ϕ) increases, the constraint contribution, f_c, should decrease and eventually vanish (eq 8, $\phi \rightarrow \infty$).

The Flory theory[6] considers topological interactions among junctions and chains only in that they restrict junction fluctuations. Ferry,[8] Langley,[9] and Dossin and Graessley[10] have argued that in the limit of *small strain* these interactions are also present along the chain contour and contribute directly to the modulus. Their conclusions are based on the rubbery plateau modulus, G_N^0, which is observed for high molecular weight linear polymers in dynamic mechanical testing. This plateau modulus is believed to be a measure of topological interactions or entanglements between chains. During network formation, a portion of these entanglements are permanently trapped, resulting in a small-strain modulus greater than that due to chemical cross-linking alone.

Dossin and Graessley[10] suggest that

$$G = \nu kT(1 - 2h/\phi)(V/V_0)^{2/3}/V + T_eG_e^{max} \quad (10)$$

where G is the small-strain modulus ($\alpha \rightarrow 1$), T_e is the fraction of the maximum concentration of topological interactions, G_e^{max}, which are permanently trapped by the network, and h is an empirical constant between one and zero, depending on the extent to which the junction fluctuations are impeded in the network ($h = 0$ for affine behavior, $h = 1$ for phantom behavior). Thus eq 10 predicts a small-strain modulus greater than that predicted by the Flory theory due to the $T_eG_e^{max}$ term.

T_e is equivalent to the probability that any pair of interacting units are each part of elastically effective chains. Therefore, it should be a definite function of the extent to which the α,ω-divinyl-PDMS chains are reacted into the network. Past work[1,2,11] has provided very strong support for this entanglement theory, using networks in which the network formation reaction (eq 1) goes nearly to completion ($\epsilon > 0.9$). The present study addresses the elastic properties of networks with progressively lower extents of cross-linking ($0.4 < \epsilon < 0.95$), with the intention of further evaluating the competing theories presented above. The experimental procedures and results are summarized in the following sections.

Experimental Section

Multifunctional poly(dimethylsiloxane) networks were prepared via the addition of a silane hydrogen on poly(methylsiloxanes) to vinyl-terminated linear PDMS polymers in the presence of *cis*-dichlorobis(diethyl sulfide)platinum(II) catalyst (see eq 1). The networks for this study were formed by employing five different molecular weights of α,ω-divinyl-PDMS: 9320, 11 100, 17 400, 21 600, and 28 100. The 9320 and 28 100 molecular weight polymers were obtained from General Electric Co.,[12] the 11 100

and 21 600 polymers were supplied by Dow Corning Co.[13], and the 17 400 molecular weight polymer was specially synthesized. Details of this synthesis and the characterization of all five α,ω-divinyl-PDMS are reported in detail elsewhere.[1,14]

The junction material, PMHS, was obtained from the fractionation of a commercial linear polymer (Aldrich Chemical Co.), $M_n \sim 3000$. The details of this procedure are also given elsewhere.[1,14] The PMHS had an intrinsic functionality ϕ_0 of 43.9 ($M_n = 2780$). The equivalent weight, E_j, is the ratio of ϕ_0 to M_n and was equal to 63.4 g/mol of silane hydrogen. *cis*-Dichlorobis(diethyl sulfide)platinum(II) catalyst was prepared as described in ref 15. The solid catalyst was dissolved in toluene to give a 1.5 wt % solution.

The two polymeric network precursors were combined with sufficient catalyst to give a 20-ppm Pt concentration. A qualitative control over the extent of cross-linking was gained by varying the molar ratio, R, of silane hydrogen to vinyl end groups. To obtain networks in which the network formation reaction was driven to near completion (high extents of cross-linking, $\epsilon > 0.9$), R was made slightly greater than unity (excess silane hydrogens).[1,14] Networks with lower values of ϵ were prepared by systematically decreasing R below unity. The unreacted vinyl groups remaining in these networks are essentially nonreactive under ambient conditions.[16]

The liquid mixture was poured into rectangular acrylate molds, degassed, and cured at 25 °C under argon for at least 14 days to ensure complete reaction. The resulting films had a thickness of 1–2 mm. Samples of each network were extracted with benzene to determine the mass fraction of polymer not incorporated into the network, w_e. The molecular weight distribution of each sol was determined by gel permeation chromatography (GPC).

For the networks prepared from the four commercial α,ω-divinyl-PDMS, these distributions were bimodal, with a high molecular weight peak due to the unreacted α,ω-divinyl-PDMS and a low molecular weight peak due to nonreactive low molecular weight PDMS (weight fraction of nonreactive PDMS, w_n, ~ 0.03).[1,11,14] The ratio of the α,ω-divinyl-PDMS peak area to the total area was multiplied by w_e to arrive at w_s, the corrected sol due only to unreacted α,ω-divinyl-PDMS. The GPC of sols from the networks prepared from the $M_n = 17\,400$ α,ω-divinyl-PDMS displayed but a single peak, identical with the GPC of the unreacted α,ω-divinyl-PDMS ($w_e = w_s$).

The extent of reaction of the terminal vinyl groups in each network, ϵ, was calculated from w_s:

$$w_s = \frac{(1-\epsilon)^2 M_n (1-w_n)}{M_n + 2RE_j} \tag{11}$$

Equation 11 assumes w_s consists only of unreacted α,ω-divinyl-PDMS; i.e., all the PMHS junction precursor is incorporated into the networks. Previously reported experimental data[1] and calculations[14] have demonstrated the validity of this assumption. Equation 11 follows from the derivations of Miller and Macosko[17] and applies only in the case of high-functionality networks ($\phi > 7$).[14]

Equilibrium swelling in benzene was determined for each network according to standard procedures.[18] The volume fraction of polymer at equilibrium swelling, v_{2m}, was calculated assuming additivity of volumes.

Equilibrium tensile stress–strain isotherms were obtained at 25 °C on dumbbell-shaped specimens (3 × 1 × 0.1 cm test regions) cut from unextracted films of the network. Samples were stressed by hanging different weights. Elongation was measured with a Gaertner cathetometer between two marks 2.9 cm apart. Measurements were made in a sequence of increasing elongations, with frequent values taken out of sequence to check reproducibility. The data were fit to a Mooney–Rivlin plot by a linear least-squares regression.

Reproducibility of the synthesis techniques was often checked by preparing duplicate films of a network and comparing their stress–strain isotherms. The precision of the testing procedures was also checked by running duplicate or triplicate samples from the same film. In both cases, good agreement was obtained (±5% for $2C_1$ and $2C_2$). For every network, duplicate or triplicate samples were tested, and the average values for $2C_1$ and $2C_2$ are reported herein. In general, the standard deviation of these average moduli was less than 5%.

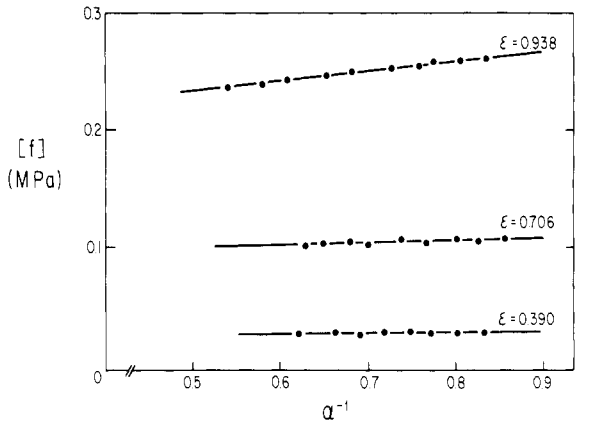

Figure 1. Representative stress–strain isotherms of end-linked PDMS networks obtained in elongation at 25 °C. Networks prepared using $\phi_0 = 43.9$ PMHS and $M_n = 21\,600$ α,ω-divinyl-PDMS at three different extents of the network formation reaction (ϵ).

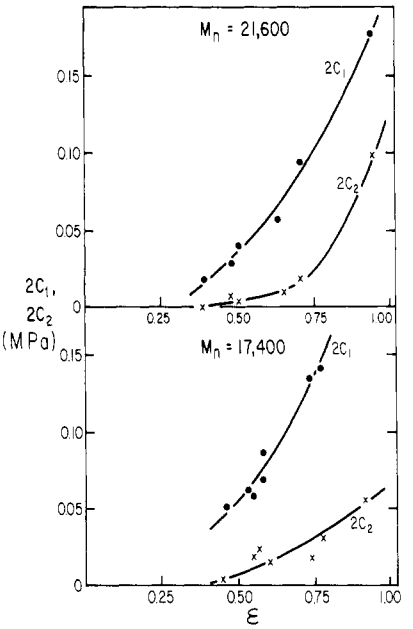

Figure 2. Dependence of the Mooney–Rivlin constants on extent of cross-linking for $M_n = 21\,600$ and 17 400 PDMS networks (●) $2C_1$; (×) $2C_2$).

The characterization data obtained for the networks prepared for this study are summarized in Table I. Listed are the M_n of the α,ω-divinyl-PDMS, the molar ratio of silane hydrogen to vinyl (R), the values of w_s, w_e, and v_{2m} in benzene, and the average values of $2C_1$ and $2C_2$. The values of ϵ as calculated from w_s are also reported in Table I.

Results and Discussion

Figure 1 is a plot of the stress–strain data for three high-functionality networks formed from the same α,ω-divinyl-PDMS ($M_n = 21\,600$) and PMHS ($\phi_0 = 43.9$) but differing in the extent of the network formation reaction as indicated on the figure. The stress–strain isotherms are plotted as reduced stress (MPa) vs. reciprocal elongation and are representative of all the networks tested in this study in their excellent agreement with the empirical Mooney–Rivlin relationship.

In Figure 1, both the small-strain ($2C_1 + 2C_2$) and the large-strain ($2C_1$) moduli are observed to decrease significantly with decreasing values of ϵ. This phenomenon is explored in greater detail in Figure 2 wherein the Mooney–Rivlin constants are plotted against ϵ for networks

Table I
Network Characterization Data and Calculations

M_n	R	ϵ	$w_e \times 100$	$w_s \times 100$	v_{2m}	$2C_1$, MPa	$2C_2$, MPa	$\phi_0\epsilon^2/R$
9 320	1.205	0.969	3.26	0.09	0.401	0.435	0.098	34.2
9 320	1.121	0.919	4.00	0.63	0.403	0.357	0.073	33.1
9 320	0.979	0.745	9.34	6.23	0.331	0.168	0.356	24.9
9 320	0.954	0.742	9.75	6.37	0.327	0.154	0.068	25.3
9 320	0.927	0.708	11.5	8.22	0.317	0.162	0.032	23.7
9 320	0.864	0.546	17.7	15.6	0.274	0.129	0.000	15.2
11 100	1.201	0.932	3.50	0.46	0.355	0.316	0.053	31.8
11 100	1.106	0.717	11.2	7.68	0.297	0.143	0.041	20.4
11 100	1.006	0.619	17.9	13.9	0.261	0.109	0.000	16.7
11 100	0.980	0.602	19.1	15.2	0.249	0.102	0.000	16.2
11 100	0.959	0.586	20.5	16.4	0.234	0.080	0.000	15.7
11 100	0.920	0.532	24.3	21.6	0.233	0.074	0.005	13.5
17 400	1.652	0.926	0.52	0.52	0.294	0.200	0.056	22.8
17 400	1.150	0.778	4.88	4.88	0.284	0.142	0.030	23.1
17 400	1.104	0.750	6.20	6.20	0.272	0.133	0.019	22.4
17 400	1.004	0.604	15.6	15.6	0.234	0.087	0.014	16.0
17 400	0.992	0.547	20.2	20.2	0.219	0.064	0.019	13.2
17 400	0.932	0.571	18.3	18.3	0.221	0.062	0.025	15.4
17 400	0.850	0.466	28.4	28.4	0.190	0.052	0.002	11.2
21 600	1.359	0.938	3.84	0.38	0.304	0.180	0.104	28.4
21 600	1.166	0.706	11.7	8.29	0.237	0.094	0.020	18.8
21 600	1.049	0.625	17.5	13.5	0.201	0.059	0.012	16.4
21 600	0.950	0.509	25.5	23.2	0.175	0.042	0.004	12.0
21 600	0.939	0.472	28.2	26.8	0.167	0.031	0.008	10.4
21 600	0.832	0.390	36.5	35.8	0.136	0.023	0.000	8.0
28 100	1.450	0.942	3.92	0.33	0.297	0.175	0.109	26.9
28 100	1.152	0.657	14.0	11.3	0.223	0.076	0.021	16.5
28 100	1.038	0.575	19.5	17.4	0.188	0.047	0.021	14.0
28 100	0.921	0.414	30.7	33.1	0.151	0.033	0.003	8.2
28 100	0.882	0.401	33.7	34.6	0.134	0.024	0.000	8.0
28 100	0.867	0.424	32.1	31.9	0.149	0.032	0.000	9.1

formed from the M_n = 21 600 and 17 400 α,ω-divinyl-PDMS. This plot is typical of the results for each molecular weight of α,ω-divinyl-PDMS used in this study (see Table I). As can be seen, both $2C_1$ and $2C_2$ decrease dramatically with decreasing ϵ.

All of the networks in this study were prepared by using a PMHS of intrinsic functionality, ϕ_0, 43.9. At low extents of the network formation reaction, the actual network functionality, ϕ, will be significantly lower than ϕ_0. ϕ may be approximated by $\phi_0\epsilon^2/R$. This approximation is a simplification of the network parameter calculations of Miller and Macosko[17] and gives excellent agreement (<0.5% error) with those calculations for $\phi_0\epsilon^2/R > 7$.[14] The calculated values of $\phi_0\epsilon^2/R$ are reported in Table I and in all cases are greater than 8.

For networks with $\phi > 10$, the Flory theory[6] would predict

$$2C_1 \sim \nu_s kT(V/V_0)^{2/3}/V \tag{12}$$

where ν_s is the number of network chains calculated from the stoichiometry of the network formation reaction (eq 1). This prediction follows from eq 7 and 8 in the limit of high-functionality networks.

For $\phi > 7$, ν_s/V may be calculated by[1,14]

$$\nu_s/V = \frac{\epsilon^2\rho}{M_n + 2RE_j} \tag{13}$$

where ρ is the density of the PDMS network. Since ν_s/V and, thus, $2C_1$ are proportional to ϵ^2, the observed ϵ dependency of $2C_1$ in Figure 2 is in qualitative agreement with the Flory theory.

However, the magnitude of $2C_2$ in Figure 2 is in discord with the Flory theory. The theory holds that the ratio f_c/f_{ph} should be essentially zero for high-functionality networks (eq 8). Thus, the modulus of these networks would be predicted to be independent of strain (eq 7). $2C_2$, being a measure of the strain dependence of the modulus, should, therefore, be immeasurably different from zero for the high-functionality networks represented in Figure 2. The data in Table I and Figures 1 and 2 emphasize that this is not so. $2C_2$ is actually measurably larger than zero even at ϵ = 0.60. Furthermore, $2C_2$ is seen to regularly decrease, much like $2C_1$, with decreasing ϵ.

The magnitudes of $2C_1$ and $2C_2$ may be evaluated more quantitatively in terms of the structure factors A_1 and A_2. These structure factors relate the small-strain (A_1) and large-strain (A_2) moduli to the number of network chains per unit volume as calculated from stoichiometry, ν_s/V, and are defined as follows:

$$A_1 = (2C_1 + 2C_2)\left[\frac{\nu_s kT}{V}(V/V_0)^{2/3}\right]^{-1} \tag{14}$$

$$A_2 = 2C_1\left[\frac{\nu_s kT}{V}(V/V_0)^{2/3}\right]^{-1} \tag{15}$$

According to the Flory theory,[6] the predicted range on A_1 and A_2 lies between 1 and $1 - 2/\phi$. The upper limit, unity, corresponds to affine behavior and the lower limit occurs in phantom behavior. Therefore both A_1 and A_2 have predicted asymptotes of 1 at high functionalities and should be independent of ν_s/V.

The small- and large-strain structure factors are plotted against ϵ in Figure 3 for networks prepared with the M_n = 21 600 and 11 100 α,ω-divinyl-PDMS. A_1 and A_2 were calculated under the assumption that $V_0 = V$. Since the networks were both formed and tested in bulk, $V = V_f \simeq V_0$ (V_f = volume of the network during formation). Both A_1 and A_2 are everywhere greater than the Flory theory predicted value of unity, approaching it asymptotically only as $\epsilon \to 0$. The ratio $A_2/A_1 = 2C_1/(2C_1 + 2C_2)$ is also plotted in Figure 3 and is seen to asymptotically increase from fractional values toward unity in the limit of low ϵ.

A third structure factor, A_3, is also plotted in Figure 3. A_3 is the ratio of network chain density calculated from

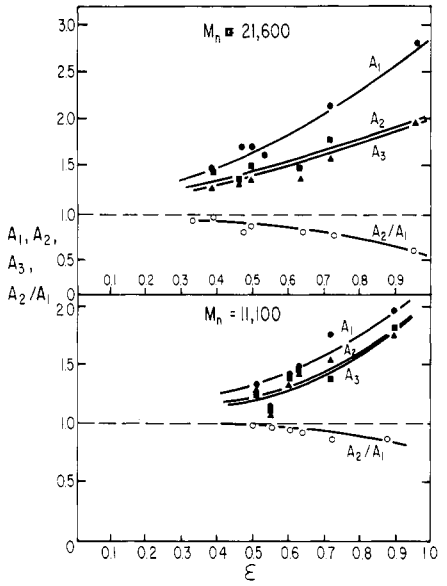

Figure 3. Dependence of A_1, A_2, A_3, and A_2/A_1 on extent of cross-linking for M_n = 21 600 and 11 100 PDMS networks ((●) A_1; (■) A_2; (▲) A_3; (○) A_2/A_1).

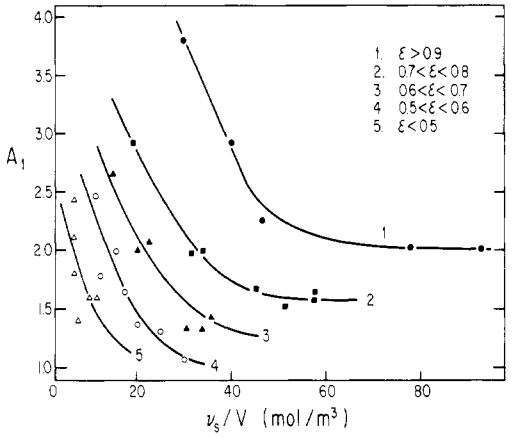

Figure 4. Dependence of A_1 on network chain density of end-linked high-functionality PDMS elastomers, $0.4 < \epsilon < 0.95$.

the affine network equilibrium swelling theory (inside the brackets) to that obtained from stoichiometry:

$$A_3 = \left[\frac{-(\ln(1 - v_{2m} + v_{2m} + \chi_1 v_{2m}^2)v_{2r}}{V_1(v_{2m}^{1/3}v_{2r}^{2/3} - 2Rv_{2m}/\phi_0\epsilon^2)}\right](V_0/\nu_s) \quad (16)$$

where $v_{2r} = V_d/V_0$, V_d is the volume of the dried extracted network, V_1 is the molar volume of the solvent, and χ_1 is the polymer–solvent interaction parameter.[4] The equilibrium swelling in benzene was used in the calculation of A_3. χ_1 was obtained as a function of volume fraction polymer from published results.[20] Good agreement is observed between A_2 and A_3 in Figure 3, suggesting a similarity between tensile and swelling behavior.

Prior research[1,2,14] showed that these three structure factors displayed a regular decreasing tendency with increasing ν_s/V for networks with $\epsilon > 0.9$. This phenomenon is explored further in Figure 4, in which the dependence of A_1 on network chain density is indicated for five different extents of the network formation reaction. In each case, the A_1 decreases asymptotically as ν_s/V increases (M_n decreases), approaching unity only for small conversions or for large values of ν_s/V. Furthermore, the rate of convergence to the asymptote increases dramatically as ϵ decreases.

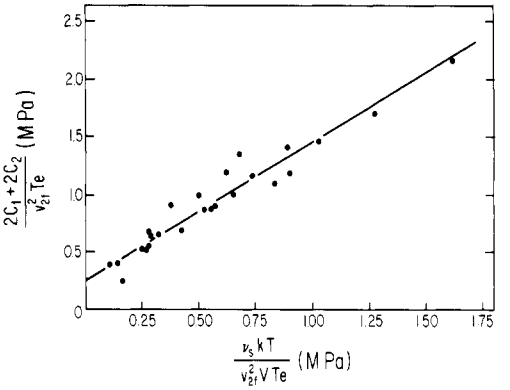

Figure 5. Langley–Graessley plot for end-linked high-functionality PDMS elastomers, $0.4 < \epsilon < 0.95$.

The observed trends in A_1 with ν_s/V and ϵ are in excellent qualitative agreement with the Langley[9]–Graessley[10,21] small-strain theory. According to eq 10 and 14 (for $\phi > 8$)

$$A_1 = \frac{(2C_1 + 2C_2)V(V_0/V)^{2/3}}{\nu_s kT} \simeq \frac{GV(V_0/V)^{2/3}}{\nu_s kT} \simeq 1 + \frac{T_e G_e^{max} V(V_0/V)^{2/3}}{\nu_s kT} \quad (17)$$

The trapping factor, T_e, is equivalent to the probability that any pair of interacting chains are both elastically effective[21] and may be calculated by using the network parameter calculations of Macosko and Miller.[17,19] T_e may be approximated by ϵ^4 with less than 0.1% error[14] when $\phi_0\epsilon^2/R > 7$. Substituting ϵ^4 for T_e, eq 13 for ν_s/V, and $V = V_0$ into eq 17 yields

$$A_1 = 1 + \epsilon^2 G_e^{max}(M_n + 2RE_j)/\rho \quad (18)$$

Therefore, the Langley–Graessley small-strain theory predicts A_1 to be everywhere greater than unity, approaching it as an asymptote as ϵ and M_n decrease.

In a recent paper,[2] Meyers and Merrill explored the effect that diluent present during network formation had on the small-strain modulus. As a consequence of that work, a modification of the Langley–Graessley small-strain theory was suggested:[2,14]

$$G = \nu_s kT(V/V_0)^{2/3}/V + T_e v_{2f}^2 v_t^{5/6}(G_e^{max})^0 \quad (19)$$

wherein $v_{2f} = V_d/V_f$, $v_t = V_f/V$, and $(G_e^{max})^0$ is the absolute maximum entanglement contribution to the small-strain modulus. This maximum would be obtained for a network formed and tested in bulk and in which all entanglements had been trapped ($v_{2f} = v_t = T_e = 1$). Equation 19 considers the effects of solvent present during network formation (v_{2f}^2) and testing as well as the effect the removal of this solvent ($v_t^{5/6}$) has on the small-strain modulus.

For the networks prepared in the current study, $V = V_f$ and $v_t = 1$. Furthermore, the networks were prepared in bulk; i.e., no external diluent was present during network formation. However, at low extents of the network formation reaction, an appreciable fraction of the α,ω-divinyl-PDMS will not be incorporated into the network. This unreacted α,ω-divinyl-PDMS acts as an "internal" diluent and is accounted through the v_{2f}^2 term in eq 19 ($v_{2f} = V_d/V_f \neq 1$).

In Figure 5, the small-strain data plotted in Figure 4 are replotted as suggested by eq 19: $(2C_1 + 2C_2)/T_e v_{2f}^2$ vs. $\nu_s kT/Vv_{2f}^2 T_e$. $2C_1 + 2C_2$ was used to approximate the small-strain modulus. This approximation can lead to slightly higher values of G due to curvature in the Moo-

ney–Rivlin plots at small extensions. However, this error appears to be less than 5%.[14] The data were fit by linear regression to a single line of slope 1.17 (±0.06) and intercept 0.236 (±0.011) MPa. The Langley–Graessley small-strain theory predicts the slope of such a plot to be $1 - 2h/\phi$. For the high junction functionality occurring in our networks, the predicted slope would be unity. Therefore there is good agreement between theoretical and experimental slopes.

The intercept in Figure 5 is predicted by eq 19 to be equal to $(G_e^{max})^0$. The experimental value of 0.236 MPa is in good agreement with the literature values of (i) G_e^{max} for tri- and tetrafunctional PDMS networks formed in bulk with $\epsilon > 0.8$ (0.21–0.25 MPa[11]), (ii) G_e^{max} for high-functionality PDMS networks formed in bulk with $\epsilon \geq 0.9$ (0.215,[1] 0.24 MPa[11]), and (iii) $(G_e^{max})^0$ for high-functionality networks prepared in the presence of diluent (0.27 MPa[2]). The value of the intercept is also in good agreement with values of G_N^0 reported in the literature for high molecular weight linear PDMS polymers (0.24, 0.20, 0.30 MPa).[2,22,23]

The values of the large-strain structure factor (A_2) for the networks tested in this study are all greater than unity but are less than the corresponding values of A_1. If the magnitudes of A_2 in excess of unity are also attributed to trapped entanglements, it would appear that the entanglement contribution to the modulus is strain dependent and decreases with increasing elongation.

Since the entanglement contribution to the modulus, G_e, is dependent on $\epsilon^4(T_e)$ while the chemical contribution G_c is dependent on $\epsilon^2(\nu_s/V)$, G_e should decrease more rapidly than G_c as ϵ is decreased. The equality of A_1 and A_2 to unity for high-functionality networks in the limit of $\epsilon \rightarrow 0$ ($G_e/G_c \rightarrow 0$) suggests that the Flory theory, in its present form, holds in the absence of trapped entanglements. Therefore, a reconsideration of the Flory theory accounting for the direct strain-dependent contribution of trapped entanglements to the modulus over the entire range of strain and ϵ is recommended.

Conclusions

The degree of agreement between the predictions of the Langley–Graessley small-strain theory and the data reported here offers significant evidence favoring a contribution to the small-strain modulus by trapped entanglements. The magnitude of A_2 suggests a strain-dependent entanglement contribution to the large-strain modulus as well.

Acknowledgment. These studies were supported by the Carbon P. Dubbs Professorship of Chemical Engineering at the Massachusetts Institute of Technology.

References and Notes

(1) Meyers, K. O.; Bye, M. L.; Merrill, E. W. *Macromolecules* **1980**, *13*, 1045.
(2) Meyers, K. O.; Merrill, E. W. In "Elastomers and Rubber Elasticity"; Mark, J. E.; Ed. (*ACS Symp. Ser.*, in press).
(3) Mooney, M. *J. Appl. Phys.* **1948**, *19*, 434. Rivlin, R. S. *Philos. Trans. R. Soc. London, Ser. A* **1948**, *241*, 379.
(4) Flory, P. J. "Principles of Polymer Chemistry"; Cornell University Press: Ithaca, N.Y., 1953.
(5) James, H. M.; Guth, E. *J. Polym. Sci.* **1949**, *4*, 153.
(6) Flory, P. J. *J. Chem. Phys.* **1977**, *66*, 5720.
(7) Ronca, G.; Allegra, G. *J. Chem. Phys.* **1975**, *63*, 4990.
(8) Ferry, J. D. "Viscoelastic Properties of Polymers", 2nd ed.; Wiley: New York, 1979.
(9) Langley, N. P. *Macromolecules* **1968**, *1*, 348.
(10) Dossin, L. M.; Graessley, W. W. *Macromolecules* **1979**, *12*, 123.
(11) Gottlieb, M.; Macosko, C. W.; Benjamin, G. S.; Meyers, K. O.; Merrill, E. W. *Macromolecules* **1981**, *14*, 1039.
(12) We are indebted to Dr. John Razzano of the General Electric Co., Silicones Division, for supplying the 9320 and 28 100 molecular weight α,ω-divinyl-PDMS.
(13) We are indebted to Professor Christopher Macosko of the University of Minnesota, Minneapolis, Minn., for providing the 11 100 and 21 600 molecular weight α,ω-divinyl-PDMS.
(14) Meyers, K. O. Doctoral Dissertation, Massachusetts Institute of Technology, Cambridge, Mass., 1980.
(15) Kauffman, C. B.; Cowan, D. O. *Inorg. Synth.* **1969**, *6*, 214.
(16) Noll, W. "Chemistry and Technology of Silicones"; Academic Press: New York, 1968.
(17) Miller, D. R.; Macosko, C. W. *Macromolecules* **1976**, *9*, 206.
(18) Collins, E. A.; Bares, J.; Billmeyer, F. W. "Experiments in Polymer Science"; Wiley: New York, 1974; p 152.
(19) Valles, E. W.; Macosko, C. W. *Macromolecules* **1979**, *12*, 673.
(20) Flory, P. J.; Tatara, Y. *J. Polym. Sci.* **1975**, *13*, 683.
(21) Pearson, D. S.; Graessley, W. W. *Macromolecules* **1980**, *13*, 1001.
(22) Plazek, D. S.; Dannhauser, W.; Ferry, J. D. *J. Colloid Sci.* **1961**, *16*, 101.
(23) Langley, N. R.; Ferry, J. D. *Macromolecules* **1968** *1*, 353.